UK/92-05
Dec. 1992
hep-lat/9304011

Nucleon Axial Form Factor from Lattice QCD

arXiv:hep-lat/9305025v1 27 May 1993

K.F. Liu, S.J. Dong, T. Draper, and J.M. Wu *

Dept. of Physics and Astronomy
Univ. of Kentucky, Lexington, KY 40506

W. Wilcox

Physics Dept., Baylor Univ., Waco, TX 76798

Abstract

Results for the isovector axial form factors of the proton from a lattice QCD calculation are presented for both point-split and local currents. They are obtained on a quenched $16^3 \times 24$ lattice at $\beta = 6.0$ with Wilson fermions for a range of quark masses from strange to charm. For each quark mass, we find that the axial form factor falls off slower than the corresponding proton electric form factor. Results extrapolated to the chiral limit show that the q^2 dependence of the axial form factor agrees reasonably well with experiment. The axial coupling constant g_A calculated for the local and the point-split currents is about 6% and 12% smaller than the experimental value respectively.

PACS numbers: 12.38 Gc, 14.20 Dh, 13.60.-r

* Present address: Institute of High Energy Physics, Beijing, China

As have electromagnetic form factors, the isovector axial form factor $g_A(q^2)$ has been commonly used to constrain the construction of models of the nucleon in order to incorporate PCAC and the Goldberger-Treiman relation [1, 2]. Similar to vector meson dominance in electromagnetic form factors, the isovector axial form factor seems to be quite sensitive to whether degrees of freedom in the A_1 channel (e.g. $\rho\pi, \omega\pi\pi$ or A_1 itself) are introduced in the effective theory [3, 4, 5]. In view of the fact that the EM form factors and the magnetic moments of the nucleon in recent lattice QCD calculations are within 10 to 15% of the experimental results [6, 7], it is natural to extend the study to the axial form factor and to determine to what extent the experimental results can be reproduced in lattice QCD, subject to the limitations of the quenched approximation, finite size effects and the extrapolation to the chiral limit. Especially interesting is to check the q^2 dependence of the axial vs. the electric form factors to see if the experimental difference between them is borne out in the lattice calculation; the q^2 dependence of their ratio should be fairly independent of the systematic errors due to the present limitations of the lattice calculation. In this paper, we study the axial form factor in lattice QCD with Wilson fermions and compare it to the electric form factor calculated previously and to experiment. We examine its systematics as a function of the quark mass from strange to twice that of the charm mass, and compare the axial coupling constant g_A to previous quenched calculations with different volumes [8, 9, 10, 11]. Fixing g_A to the non-relativistic value of 5/3, we determine the finite lattice renormalization for heavy quarks. Assuming axial dominance, we extract the A_1NN form factor.

Lattice gauge calculations have been carried out to study the electromagnetic form factors of the pion[12] and the nucleon[6, 7]. The same sequential source technique (SST) using the zero-momentum point nucleon interpolating field as the secondary source is applied here to study the axial form factors [7]. In choosing the final hadron as the secondary source, one can sew the quark propagators together at the point where the current couples in the three-point function. This has the advantage of being able to study different currents at various momentum transfers.

The lattice two- and three-point functions that we calculate are the following:

$$G_{PP}^{\alpha\alpha}(t,\vec{p}) = \sum_{\vec{x}} e^{-i\vec{p}\cdot\vec{x}} \langle 0|T(\chi^\alpha(x)\bar{\chi}^\alpha(0)|0\rangle, \tag{1}$$

$$G_{PAP}^{\alpha\beta}(t_f,\vec{p},t,\vec{q}) = \sum_{\vec{x}_f,\vec{x}} e^{-i\vec{p}\cdot\vec{x}_f + i\vec{q}\cdot\vec{x}} \langle 0|T(\chi^\alpha(x_f)A_\mu(x)\bar{\chi}^\beta(0))|0\rangle, \tag{2}$$

where χ^α is the proton interpolating field and $A_\mu(x)$ is either the point-split axial vector current

$$A_\mu^{PS} = i2\kappa[\bar{\psi}(x)\frac{1}{2}\gamma_\mu\gamma_5 U_\mu(x)\psi(x+\hat{\mu}) + \bar{\psi}(x+\hat{\mu})\frac{1}{2}\gamma_\mu\gamma_5 U_\mu^\dagger(x)\psi(x)], \tag{3}$$

or the local current

$$A_\mu^{LOC} = i2\kappa\bar{\psi}(x)\gamma_\mu\gamma_5\psi(x). \tag{4}$$

Phenomenologically, the axial vector current matrix element is written as

$$\langle \vec{p}s|A_\mu(0)|\vec{p}'s'\rangle = \bar{u}(\vec{p},s)[i\gamma_\mu g_A(q^2) - q_\mu h_A(q^2)]\gamma_5 u(\vec{p}',s'). \tag{5}$$

It has been shown [13] that when $t_f - t$ and $t >> a$, the lattice spacing, the ratio of eqs. (2) and (1) gives the following relations for the A_3 and A_4 matrix elements

$$\frac{\Gamma^{\beta\alpha}G^{\alpha\beta}_{PA_3P}(t_f,\vec{0},t,\vec{q})}{G^{\alpha\alpha}_{PP}(t_f,\vec{0})} \longrightarrow \frac{m+E_q}{2E_q}e^{-(E_q-m)t}[g_A(q^2) - \frac{q_3^2}{E_p+m}h_A(q^2)], \tag{6}$$

$$\frac{\Gamma^{\beta\alpha}G^{\alpha\beta}_{PA_4P}(t_f,\vec{0},t,\vec{q})}{G^{\alpha\alpha}_{PP}(t_f,\vec{0})} \longrightarrow \frac{q_3}{2E_q}e^{-(E_q-m)t}[g_A(q^2) + (m-E_q)h_A(q^2)], \tag{7}$$

where $\Gamma = \begin{pmatrix} \sigma_3 & 0 \\ 0 & 0 \end{pmatrix}$. When $\vec{q} = 0$, eq. (6) reduces to g_A, the coupling constant. For finite momentum transfer, $g_A(q^2)$ can be obtained from eq. (6) upon eliminating the kinematic factor extracted from the ratio of the two-point functions $G^{\alpha\alpha}_{PP}(t,\vec{q})/G^{\alpha\alpha}_{PP}(t,0)$, and by setting q_3 to zero. The only exception is when $\vec{q}^2 = 3(2\pi/La)^2$ where q_3 can not be set to zero. In this case, we use both eqs. (6) and (7) to obtain $g_A(q^2)$ at this $\vec{q}^2$.

Our quenched gauge configurations were generated on a $16^3\times 24$ lattice at $\beta = 6.0$. The gauge field was thermalized for 5000 sweeps from a cold start and 12 configurations separated by at least 1000 sweeps were used. Periodic boundary conditions were imposed on the quark fields in the spatial directions. In the time direction, the fixed (uncoupled) quark boundary condition was used. All quark propagators were chosen to originate from lattice time slice 5; the secondary nucleon source was fixed at time slice 20 (except for $\kappa = 0.154$ where the quark propagators from time slice 3 to 22 are used). We also averaged over the directions of equivalent lattice momenta in each configuration; this reduces error bars.

The results presented here are for Wilson fermions with $\kappa = 0.154$, 0.152, 0.148, 0.140, 0.133, 0.120 and 0.105 so that a range of quark masses from the strange to about twice the charm mass is covered. To extract the lattice axial charge g_A^L, instead of using the ratio in eq. (6), we fit the three-point and two-point functions to two exponentials in the form of $g_A^L f e^{-mt}$ and $f e^{-mt}$ simultaneously using the data-covariance matrix to account for the fact that they are measured on the same set of gauge configurations [14]. The range of t for the two-point functions are chosen to overlap with the t_f in the three-point function. This is done except for the heavy masses (i.e. $\kappa = 0.120$ and 0.105 for the point-split current and 0.140 and 0.133 in addition for the local current) where eq. (6) is used. For $q^2 \neq 0$, we used the combined ratios in eqs. (6) and (7) and $G^{\alpha\alpha}_{PP}(t,\vec{q})/G^{\alpha\alpha}_{PP}(t,0)$ to extract $g_A^L(q^2)$, since we do not have enough gauge configurations to warrant a simultaneous fit [15]. The errors are obtained through the jackknife in this case.

Table 1: Unrenormalized coupling constants g_A^L calculated with the point-split and the local currents for different quark masses. Also listed are the χ^2 per degree of freedom from the covariance fit.

κ	.154	.152	.148	.140	.133	.120	.105
g_A^L (point-split)	1.28(17)	1.26(6)	1.24(4)	1.11(1)	0.98(1)	0.763(7)	0.546(7)
χ^2/N_{DF}	0.28	0.03	0.77	0.43	1.3		
g_A^L (local)	1.47(18)	1.43(5)	1.40(5)	1.25(1)	1.11(1)	0.88(1)	0.651(6)
χ^2/N_{DF}	0.20	0.70	0.77				

In Table 1, we list the unrenormalized coupling constants $g_A^L = g_A^L(q^2 = 0)$ for the point-split current (P-S.C.) and the local current (L.C.) for different κ. We see that the results from the P-S.C. are lower than those of the L.C. We will address this point later.

Plotted in Fig. 1 are the unrenormalized lattice isovector axial form factors $g_A^L(q^2)$ of the proton as a function of the quark mass in dimensionless units $m_q a = \ln[1 + 1/2(1/\kappa - 1/\kappa_c)]$ for different momentum transfers $\vec{q}^2$ from 0 to 4 times $(2\pi/La)^2$ for the point-split current. (N.B. $q^2 = (E - m_N)^2 - \vec{q}^2$ for the four-momentum transfer squared.) Also included are earlier results for g_A^L from smaller lattices ($10^3 \times 20$ [9] and $12^3 \times 22$). Although error bars overlap, we note that the finite volume effect is still appreciable for the light quarks. A recent quenched calculation with the same spatial dimension ($16^3 \times 40$ with $\beta = 6.0$) [11] shows that g_A^L at large κ values of 0.154 and 0.155 for the local current are at 1.36(4) and 1.39(14). Our result of 1.47(18) for $\kappa = 0.154$ is compatible with these and is also in agreement with the earlier calculation with a renormalization improved Wilson action [10]. The extrapolation of g_A^L to the chiral limit at κ_c is carried out with the correlated fit to a linear dependence on the quark mass $m_q a$ for $\kappa = 0.154$, 0.152 and 0.148. The covariance matrix is calculated with the single elimination jackknife error for g_A^L, itself calculated from the simultaneous fit described above for different κ.

This extrapolation gives the unrenormalized g_A^L at the chiral limit to be 1.28(9) for the P-S.C. and 1.47(9) for the L.C. with $\chi^2/N_{DF} = 0.01$ for both cases. Using the finite lattice renormalization Z_L to be 0.86 for the P-S.C. [16] and 0.8 for the L.C. [17] as determined from current algebra matrix elements, the continuum g_A which equals $Z_L g_A^L$ is 1.10(8) for the P-S.C. and 1.18(7) for the local current. This is about 12% and 6% smaller than the experimental value of 1.254(6) respectively.

It was demonstrated in a previous study [9] that the lattice axial charge g_A^L for the Wilson action is $(5/3)2\kappa$ for the L.C. and $\sim \kappa^2$ for the P-S.C. at the static limit. A quark mass dependent factor $f(m_q a) = e^{m_q a} = 1 + 1/2(1/\kappa - 1/\kappa_c)$ has been

Table 2: Renormalization factor Z_A^L for the heavy quarks

κ	.140	.133	.120	.105
Z_A^L (local)	0.98(1)	0.97(1)	0.97(1)	1.00(1)
Z_A^L (point-split)	1.10(1)	1.09(1)	1.11(1)	1.19(2)

introduced to local scalar [11] and axial currents [10, 11] to smoothly interpolate between the limits of $m_q \to 0$ where $f \to 1$ and $m_q \to \infty$ where $f \to 1/(2\kappa)$ so that the static limit from the Wilson action matches with the continuum results. A similar factor is found in analyzing the Wilson action for non-relativistic quarks [18]. We multiply g_A^L by this factor $e^{m_q a}$ for both the L.C. and P-S.C. and plot them in Fig. 2 as a function of the quark mass $m_q a$. It is seen that from $\kappa = 0.140$ on, the curve flattens and the value is very close to the non-relativistic quark model result of 5/3. We believe that this means the onset of the non-relativistic limit is near $\kappa = 0.140$ and additional fine tuning beyond the mean field finite lattice renormalization factor $e^{m_q a}$ is needed to bring g_A to be 5/3 for quark masses heavier than $\kappa = 0.140$. In other words, the lattice field ψ_L is related to the continuum field ψ_c through $\psi_c = (2\kappa e^{m_q a} Z_A^L)^{1/2} \psi_L$. The factor Z_A^L is listed in Table 2 for both the L.C. and the P-S.C. for the heavy quarks. To stress the fact that these κ's are *not* at the static limit, we should mention that g_A^L(local) for $\kappa = 0.105$ is $2\kappa(3.10)$ not the static value of $2\kappa(5/3)$. It is the $Z_A^L e^{m_q a}$ factor that brings it to the non-relativistic value of 5/3. It is worthwhile pointing out that the finite lattice renormalization can be done for heavy quarks in a gauge invariant way without having to renormalize to quark properties which involves gauge fixing. Z_A^L for these quark masses is found to be very close to unity for the L.C. This means that the $2\kappa e^{m_q a}$ is a satisfactory ansatz for the renormalization. Z_A^L for the P-S.C. turns out to be 10 to 20% larger. One would think that this is due to the extra gauge-field link in the P-S.C. (eq. (3)) and that replacing it with the mean field average u_0 which is between 0.8 and 0.9 at $\beta = 6$ would reconcile the difference between the Z_A^L's in these two currents. However, as we pointed out earlier, the g_A^L for the P-S.C. falls faster than that for the L.C. by an extra κ toward the static limit [9]. Hence, $Z_A^L = Z_A^L(\kappa, g)$ is a function of both κ and g. It can not be related to the mean field alone.

For $q^2 \neq 0$, we extrapolate the form factor to the chiral limit with the procedure described in Ref. [11]. The error of the linear extrapolation is calculated from the single elimination jackknife method. For each jackknife sample, the fit is carried out with the covariance matrix to calculate χ^2/N_{DF}. The average χ^2/N_{DF} turns out to be about 1 or less.

In Fig. 3, we plot the axial form factor extrapolated to the chiral limit for the L.C. and the P-S.C. in comparison with the experimental result. In doing so, we have used

the calculated nucleon mass to set the scale for the momentum as was done in ref. [7]. For comparison, we also show the calculated electric form factor G_E extrapolated to the chiral limit [7] (without the covariance matrix) and the corresponding experimental results. The experimental $g_A(q^2)$ has been measured in neutrino-neutron scattering and pion electroproduction. The neutrino data gives a good fit in the dipole form up to $q^2 = 3\text{GeV}^2/c^2$ [19], i.e. $g_A(q^2) = g_A(0)/(1 - q^2/M_A^2)^2$, with the axial vector coupling constant $g_A(0) = 1.254 \pm 0.006$ and $M_A = 1.032 \pm 0.036$GeV (world average). Our fit of the axial form factor to the dipole form yields $M_A = 1.03 \pm 0.05$GeV for the P-S.C. and $M_A = 1.03 \pm 0.03$GeV for the L.C. which are very close to the experimental dipole mass. Similarly, the fitted dipole mass for G_E is $M_E = 0.77 \pm 0.03$GeV which is close to the experimental dipole mass of 0.828 ± 0.006GeV. We should quickly point out that the favorable agreement with the experiments to a few per cent level for the dipole mass could be fortuitous at this stage since we have not adequately assessed the systematic errors due to the finite size effect, the dynamical fermion effect, etc. Especially, the isovector part of the charge radius of the nucleon has a chiral $\ln m_\pi^2$ divergence while approaching the chiral limit [20]. This correction to the lattice extrapolation to the physical pion mass can increase the charge radius by a significant amount [21]. However, unlike the isovector vector current which can couple to two π's leading to a pion loop, the isovector axial current couples to three π's. Hence, it is not subjected to the chiral $\ln m_\pi^2$ correction as alluded to for the charge form factor. Notwithstanding these corrections (e.g. finite volume, dynamical fermion, chiral limit), we want to stress the fact that the q^2 dependence of the axial form factor shows that it is harder (i.e. falls off slower) than the corresponding $G_E(q^2)$ at each quark mass we studied. This feature, shown at the chiral limit in Fig. 3, is consistent with the experimental data (i.e. the dipole mass of 1.03 GeV for the axial case is higher than the 0.828 GeV for G_E). This feature, we believe, is likely to survive the various lattice and chiral corrections.

As far as the q^2 dependence is concerned, we find that the falloff is faster as the quark mass decreases. This is evidenced in Fig. 4(a) where $g_A^L(q^2)/g_A^L(0)$ for the P-S.C. is plotted for different quark masses. This is consistent with the fact that the associated meson cloud, specifically the A_1, will have a larger Compton wavelength as the meson masses decrease with the quark mass. In view of the success of the vector dominance and the Goldberger-Treiman relation, the idea of axial dominance for the isovector axial form factor seems to work well phenomenologically [5]. With the axial dominance assumption in mind, $g_A(q^2)$ can be written as

$$g_A(q^2) \sim g_{A_1NN}(q^2)/(1 - q^2/m_{A_1}^2) \tag{8}$$

where $g_{A_1NN}(q^2)$ is the A_1NN form factor. This is calculated by $g_A^L(q^2)(1 - q^2/m_{A_1}^2)$ at $\kappa = 0.148$, 0.152, and 0.154 and extrapolated to the chiral limit. The results for the P-S.C. normalized at $q^2 = 0$, are plotted in Fig. 4(b). We see that the q^2 falloff is now less sensitive to the quark mass than the case of $g_A^L(q^2)$. Finally we fit the $g_{A_1NN}(q^2)$ obtained this way with a monopole and found a monopole mass of 1.08 ± 0.06GeV

for the P-S.C. and 1.01 ± 0.04GeV for the L.C.

To conclude, we have calculated the isovector axial form factor of the nucleon for quark masses from strange to two times the charm mass. Albeit it is a quenched approximation, we find that g_A, extrapolated to the chiral limit, is about 6% smaller than in experiment for the local current and about 12% smaller for the point-split current. It is important to include the $e^{m_q a}$ correction factor for heavy quarks. The additional finite lattice correction for the local and point-split axial currents has been determined for heavy quarks in a gauge invariant way. We note that $g_A(q^2)$ is harder than $G_E(q^2)$ of the proton which is in agreement with experiment. This finding is most likely to be preserved when finite volume, chiral, and dynamical fermion effects are included. Assuming axial vector dominance, we have extracted the $A_1 NN$ form factor. For future studies, it is essential to improve the calculation by expanding the volume and incorporating dynamical fermions.

This work is partially supported by the DOE Grand Challenge Award, DOE Grant No. DE-FG05-84ER40154 and NSF Grants No. STI-9108764 and PHY- 9203306. We would like to thank R.M. Woloshyn for providing us with his unpublished results on the $12^3 \times 22$ lattice.

References

[1] G.E. Brown and M. Rho, Phys. Lett. **82B**, 177 (1979).

[2] G. Adkins, C. Nappi, and E. Witten, Nucl. Phys. **B228**, 552 (1983).

[3] B.A. Li and K.F. Liu, Chiral Solitons, ed. K.F. Liu (World Scientific, 1987), p. 421.

[4] U.-G. Meissner, N. Kaiser, and W. Weise, Nucl. Phys. **A466**, 685 (1987).

[5] M. Gari and U. Kaulfuss, Phys. Lett. **138B**, 29 (1984).

[6] T. Draper, R.M. Woloshyn, and K.F. Liu, Phys. Lett. **B234**, 121 (1990); G. Martinelli and C. T. Sachrajda, Nucl. Phys. **B316**, 355 (1989).

[7] W. Wilcox, T. Draper, and K.F. Liu, Phys. Rev. **D46**, 1109 (1992).

[8] F. Fucito, G. Parisi, and S. Petrarca, Phys. Lett. **115B**, 148 (1982).

[9] R.M. Woloshyn and K.F. Liu, Nucl. Phys. **B311**, 527 (1988/89).

[10] S. Güsken et. al., Phys. Lett. **227B**, 266 (1989).

[11] R. Gupta et. al., Phys. Rev. **D44**, 3272 (1991).

[12] T. Draper, R.M. Woloshyn, W. Wilcox and K.F. Liu, Nucl. Phys. **B318**, 319 (1989).

[13] K.F. Liu, J.M. Wu, S.J. Dong, and W. Wilcox, Nucl. Phys. **B20** (Proc. Suppl.), 467 (1991).

[14] Y. Liang, K.F. Liu, B.A. Li, S.J. Dong, and K. Ishikawa, Phys. Lett., to appear; S. Gottlieb, W. Liu, R.L. Renken, R.L. Sugar, and D. Toussaint, Nucl. Phys. **B9** (Proc. Suppl.), 259 (1989); C. Bernard, C.M. Head, J. Labrenz, and A. Soni, Nucl. Phys. **B26** (Proc. Suppl.), 384 (1992).

[15] D. Daniel, R. Gupta, and D. Richards, Phys. Rev. **D43**, 3715 (1991).

[16] L. Maiani and G. Martinelli, Phys. Lett. **B178**, 265 (1986).

[17] S. Güsken et. al., Nucl. Phys. **B327**, 763 (1989).

[18] G. P. Lepage, Nucl. Phys. **B26** (Proc. Suppl.), 45 (1991).

[19] N. Baker *et al.*, Phys. Rev. **D23**, 2499 (1981); K. Miller *et al.*, Phys. Rev. **D26**, 537 (1982); T. Kitagaki *et al.* Phys. Rev. **D28**, 436 (1983).

[20] M.A. Bég and A. Zepeda, Phys. Rev. **D6**, 2912 (1972).

[21] D.B. Leinweber and T.D. Cohen, Phys. Rev. **D47**, 2147 (1993).

Figure Captions

Fig. 1 The unrenormalized isovector axial form factor $g_A^L(q^2)$ for the point-split current as a function of the quark mass $m_q a$. The top curve is for $q^2 = 0$, the rest are for $\vec{q}^2$ from 1 to 4 times of $(2\pi/La)^2$ in descending order.

Fig. 2 The lattice g_A^L multiplied by the finite lattice correction factor $e^{m_q a}$ for the point-split and the local currents as a function of the quark mass.

Fig. 3 The calculated $g_A(q^2)$ for the L.C. and $G_E(q^2)$ of the proton as a function of $-q^2$. The dashed line is the fit to the experimental $g_A(q^2)$ with a dipole mass of 1.03GeV. The solid curve is the same for the experimental $G_E(q^2)$ with a dipole mass of 0.828GeV.

Fig. 4 (a) $g_A^L(q^2)/g_A^L$ for the P-S.C. for different quark masses as a function of $-q^2a^2$. (b) $g_{A_1NN}(q^2)/g_{A_1NN}(0)$ defined in eq. (8) from the P-S.C. for several quark masses.

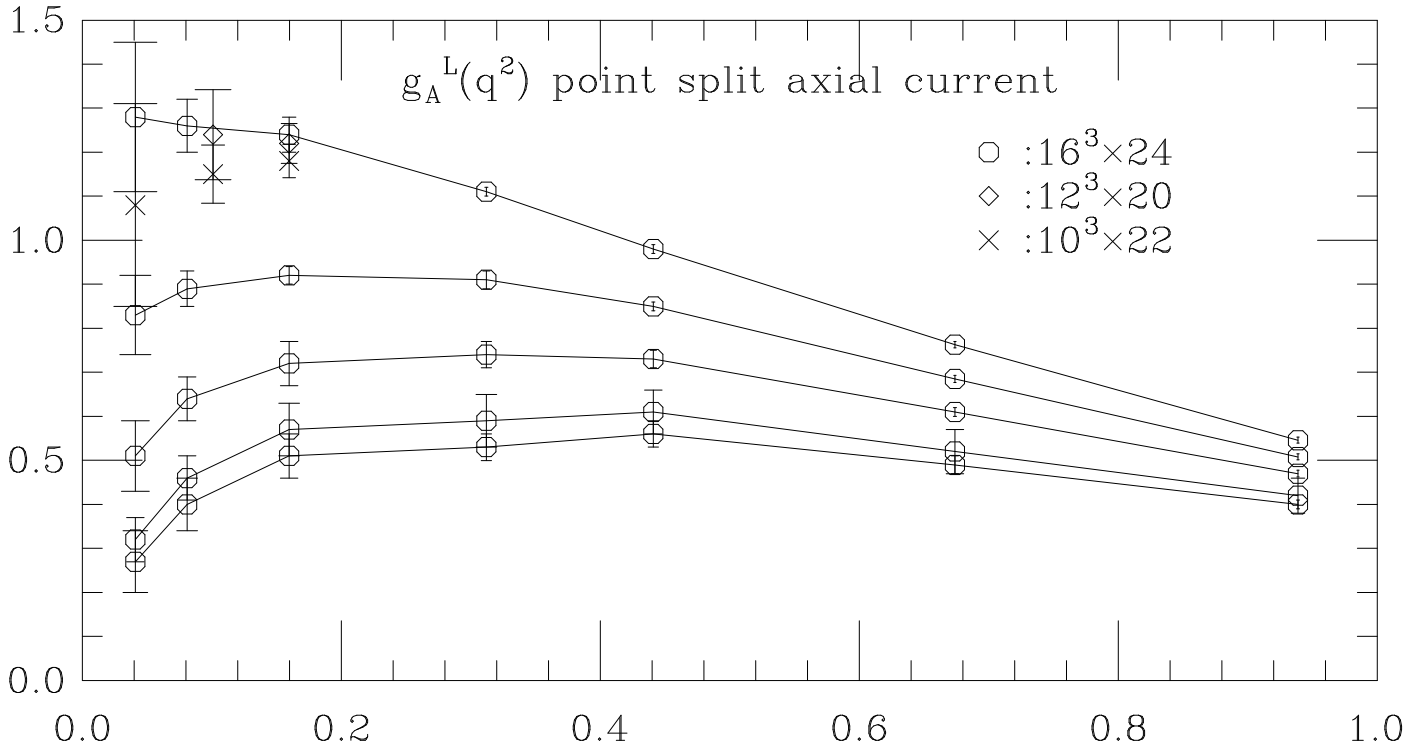

Fig.1 $m_q a=\ln(1+1/2(1/\kappa-1/\kappa_c))$

This figure "fig2-1.png" is available in "png" format from:

http://arXiv.org/ps/hep-lat/9305025v1

This figure "fig3-1.png" is available in "png" format from:

http://arXiv.org/ps/hep-lat/9305025v1

This figure "fig4-1.png" is available in "png" format from:

http://arXiv.org/ps/hep-lat/9305025v1

This figure "fig5-1.png" is available in "png" format from:

http://arXiv.org/ps/hep-lat/9305025v1

This figure "fig6-1.png" is available in "png" format from:

http://arXiv.org/ps/hep-lat/9305025v1

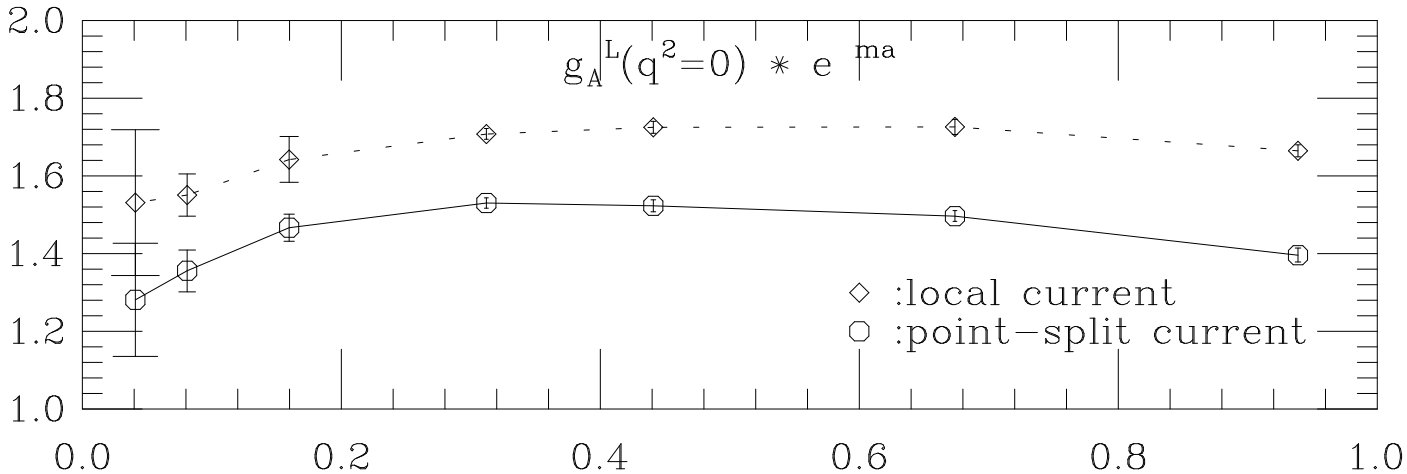

Fig.2 $m_q a = \ln(1+1/2(1/\kappa - 1/\kappa_c))$

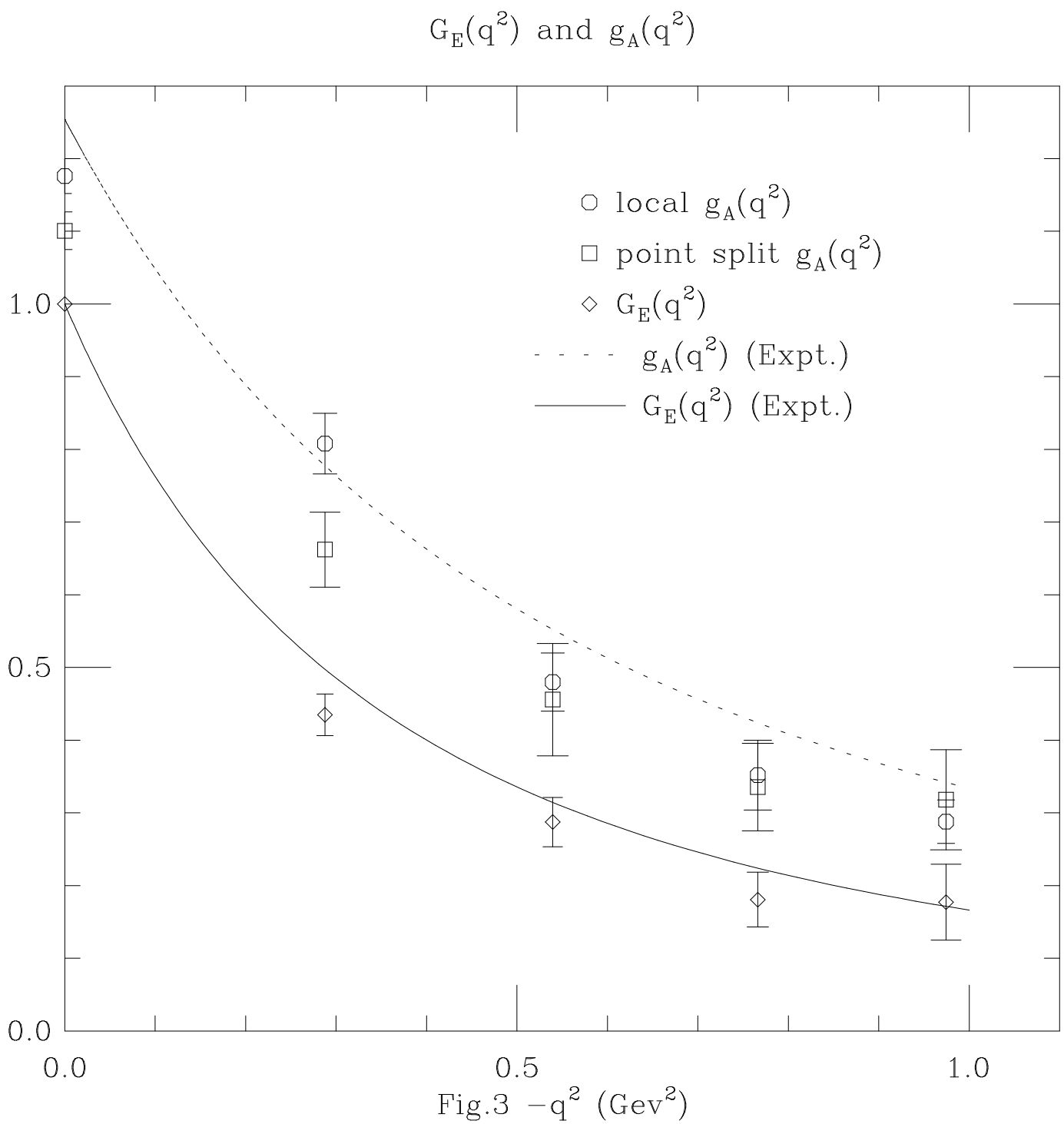
$G_E(q^2)$ and $g_A(q^2)$
local $g_A(q^2)$
point split $g_A(q^2)$
$G_E(q^2)$
$g_A(q^2)$ (Expt.)
$G_E(q^2)$ (Expt.)
1.0
0.5
0.0
0.0
0.5
1.0
$-q^2$ (Gev^2)

Fig.3

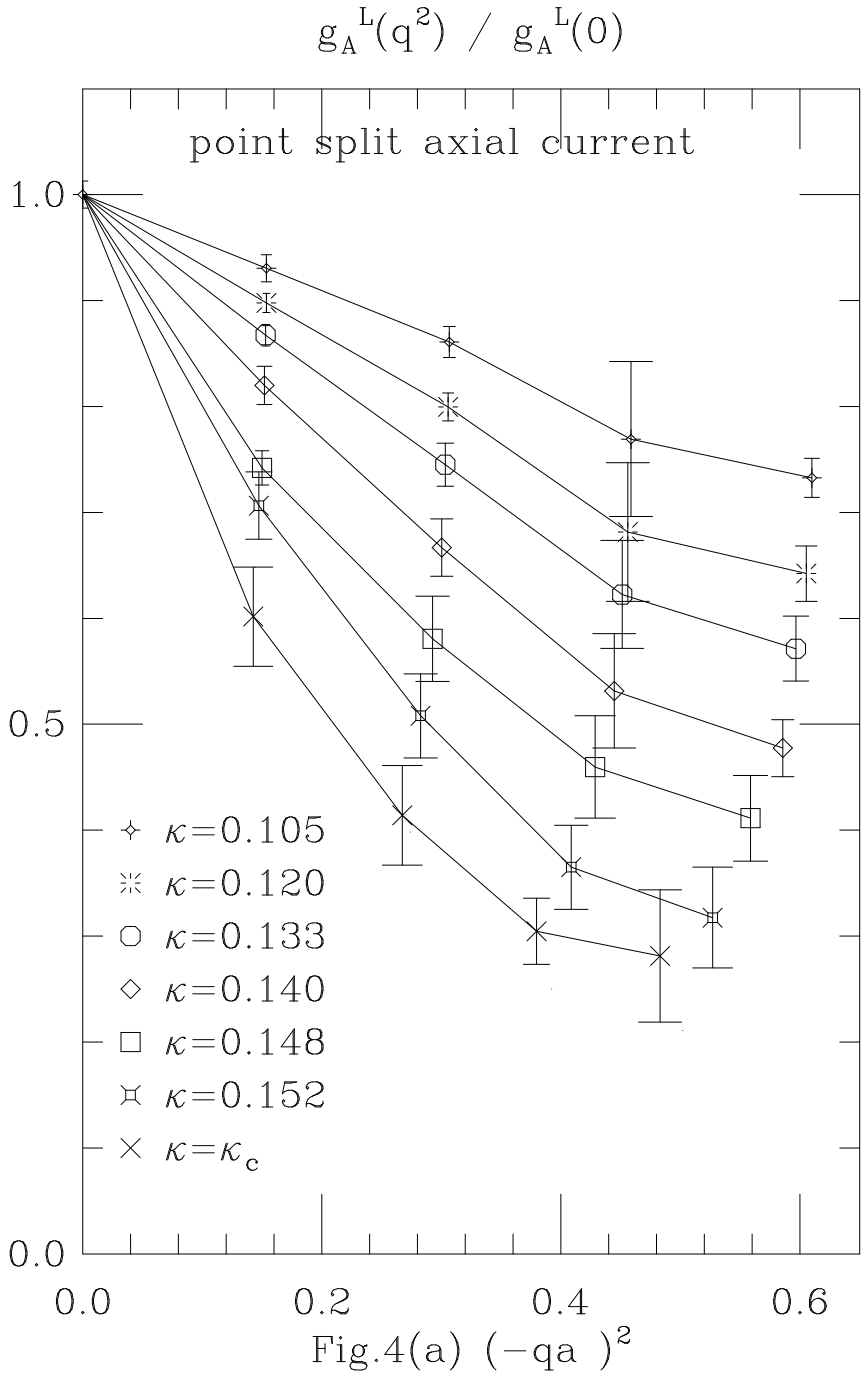
$g_A^L(q^2)\ /\ g_A^L(0)$
point split axial current
1.0
0.5
0.0
0.0
0.2
0.4
0.6
κ=0.105
κ=0.120
κ=0.133
κ=0.140
κ=0.148
κ=0.152
$\kappa=\kappa_c$
$(-qa)^2$

Fig.4(a)

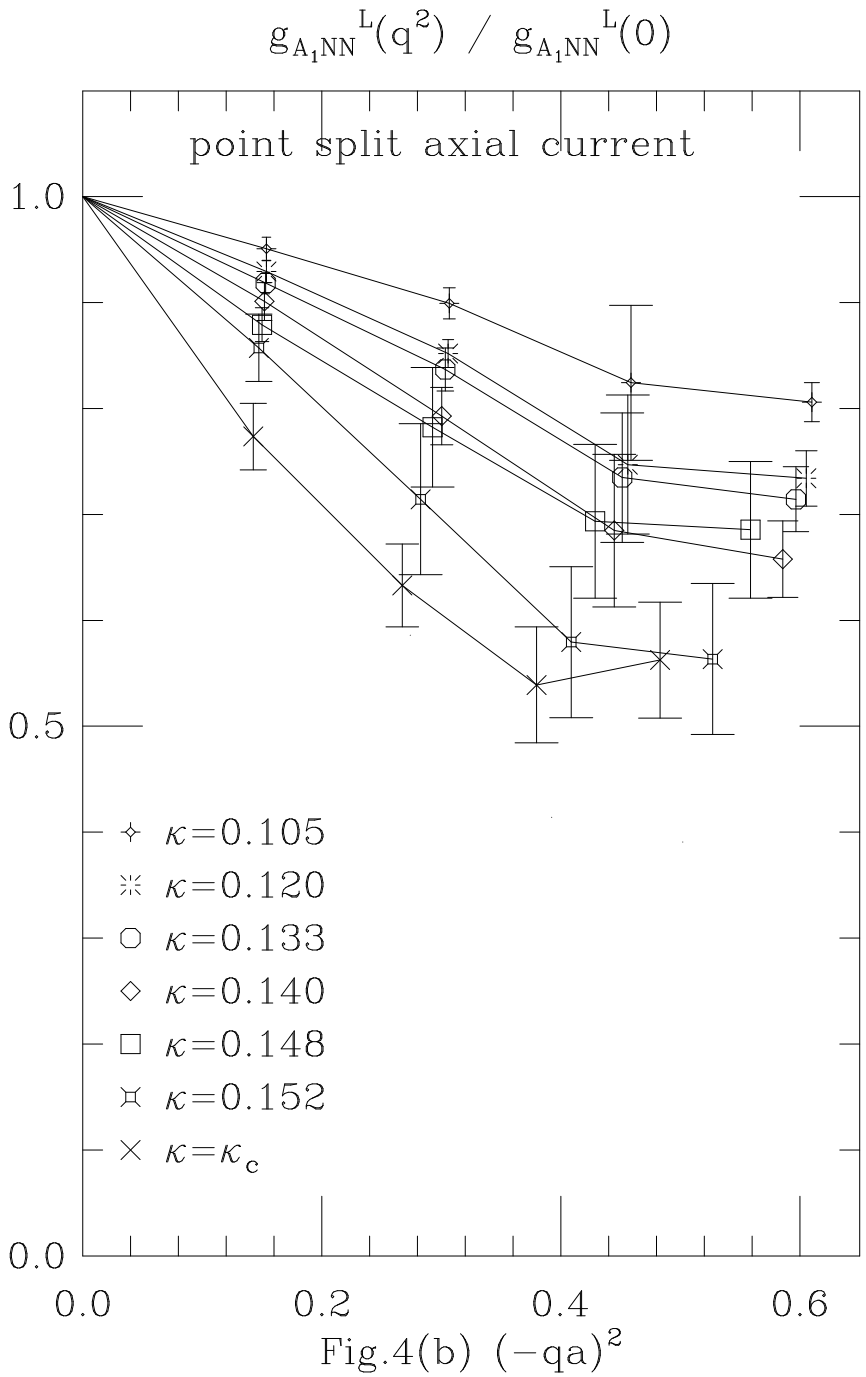
$g_{A_1NN}{}^{L}(q^2)$ / $g_{A_1NN}{}^{L}(0)$
point split axial current
1.0
0.5
0.0
0.0
0.2
0.4
0.6
κ=0.105
κ=0.120
κ=0.133
κ=0.140
κ=0.148
κ=0.152
κ=κ_c

Fig.4(b) $(-qa)^2$